

Hydrometeor type classification in winter clouds using X-band polarimetric radar measurements

Koyuru Iwanami ^{*1}, Kenichi Kusunoki ², Narihiro Orikasa ²,
Masayuki Maki ¹, Ryohei Misumi ¹, and Masataka Murakami ²

¹*National Research Institute for Earth Science and Disaster Prevention (NIED), Tsukuba, Japan*

²*Meteorological Research Institute, Tsukuba, Japan*

1. Introduction

Hydrometeor type classification in precipitation clouds is useful for not only study of precipitation mechanisms but also disaster prevention by monitoring and/or forecast of hail and lightning, discrimination between rain and snow, and improvement of weather forecast through data assimilation. Polarimetric radar measurements of precipitation can be used effectively to classify hydrometeor types in precipitation because they are sensitive to the hydrometeor properties. Hydrometeor type classification using the fuzzy logic techniques has been proposed and there are two models of the product method (Liu and Chandrasekar 2000) and the additive method (Zrnić et al. 2001) in the interference stage of fuzzy logic classification system. Recently Lim et al. (2005) proposed a hybrid model that combined the additive method and the product method.

In order to develop hydrometeor classification method using X-band polarimetric radar measurements, simultaneous observations were carried out by the NIED X-band polarimetric radar (MP-X; Iwanami et al. 2001) and the hydrometeor videosondes (HYVIS; Murakami and Matsuo, 1990) in Niigata prefecture, Japan in December 2001. Characteristics of polarimetric measurements and temperature for five hydrometeor types were derived from comparisons of the MP-X and the HYVIS data. The beta membership functions in the fuzzification process of the fuzzy logic classification were specified based on the derived characteristics of polarimetric measurements for each hydrometeor type. Results of hydrometeor classification using fuzzy logic technique including a hybrid rule strength (Lim et al. 2005) and its verification are presented.

2. Observation and data

Simultaneous observation was carried out by the NIED X-band polarimetric radar (MP-X; Iwanami et al. 2001) and the hydrometeor videosondes (HYVIS; Murakami and Matsuo, 1990) in Niigata prefecture, Japan for three weeks in December, 2001 by the National Research Institute for Earth Science and Disaster Prevention (NIED) and the Meteorological Research Institute (MRI). MP-X radar site located on the southeastern slope of the Uonuma hills. Radar data were collected in the southeastern area of the site within 30 km range.

The balloons equipped with the hydrometeor videosonde (HYVIS) and a rawinsonde were launched at the surface meteorological observation site located 2.2 km southeast from the radar site.

Main specifications of the NIED X-band polarimetric radar, MP-X (Iwanami et al. 2001), mounted on a 4-ton truck are listed in Table 1. Radar data were collected by RHI scans during HYVIS observations considering their tracks. The range and angle resolutions and number of pulse integration was 100 m, 0.5 degree and 256, respectively. The dwell time for one RHI scan was about 38 sec. The polar coordinate data by RHI scans were transformed to the Cartesian coordinate data with 500 m horizontal and 250 m vertical resolutions. Polarimetric measurements of reflectivity at horizontal polarization (Z_H), differential reflectivity (Z_{DR}) and correlation coefficient (ρ_{HV}) were mainly analyzed.

Table 1. Specifications of the NIED MP-X radar.

Frequency	9.375 GHz
Beam Width	1.3 degree
Peak Power	50 kW
Pulse Width	0.5 μ s
PRF	$\leq 1,800$ Hz
Polarization	SHV
Observation Range	≤ 80 km
Outputs	Z_H , V , W , Z_{DR} , ρ_{HV} , Φ_{DP} , K_{DP}

The hydrometeor videosonde (HYVIS) has been developed to measure the vertical distribution of hydrometeors in clouds by Murakami and Matsuo (1990). Two small TV cameras in the HYVIS take pictures of hydrometeors. The HYVIS and a rawinsonde are attached to the same balloon and launched into clouds, so that both particle images and meteorological data are collected simultaneously.

Fifteen balloons equipped with the HYVIS systems were launched during the field experiment and the data of nine HYVIS launches could be analyzed together with radar data. One-hour precipitation amounts and air temperature on the surface around their launch times were from 0 to 1.0 mm and from 0.1 to 6.9 °C, respectively.

The HYVIS data of the position, air temperature, and hydrometeor type were utilized in this analysis. Although hydrometeor types were at first classified into eight categories of water drop (R), sleet (S), graupel (G), aggregate (A), dendrite (D), column (C), plate (P), and needle (N) from the particle images, D, C, P, and N were classified into one category of single ice crystal (X) in the following analysis.

3. Characteristics of polarimetric measurements for hydrometeor types

Characteristics of polarimetric measurements of reflectivity at horizontal polarization (Z_H), differential reflectivity (Z_{DR}) and correlation coefficient (ρ_{HV}) and temperature (T) for five hydrometeor types, that is, water drop (R), sleet (S), graupel (G), aggregate (A) and ice crystal (X), were derived from comparisons of MP-X and HYVIS data.

The position of HYVIS was compared with the plane of RHI scan, then the sets of radar and HYVIS data were picked up on conditions that the time difference was less than 3 minutes and the horizontal distance between the position of the HYVIS and the plane of RHI scan was less than 1.5 km.

Table 2 shows the number of HYVIS image data for each hydrometeor type picked up for comparisons between polarimetric measurements and hydrometeor types on the conditions described above. There were a few hydrometeor types in one HYVIS image in many cases. In such cases, those different hydrometeor types were

compared with the same polarimetric parameters in one mesh on RHI data, that is, the numbers in the column ‘Multi’ in Table 2 include overlap. If another condition that there was only one type of hydrometeor in one HYVIS image was added, the numbers of HYVIS image data decreased by 4 (A) to 54 % (R) shown in the column ‘Single’ in Table 2.

Table 2. The number of HYVIS image data for each hydrometeor type. See text.

Hydrometeor Type	Number of HYVIS Image Data	
	Multi	Single
: Water Drop	485	262
S: Sleet	188	67
G: Graupel	973	198
A: Aggregate	326	12
X: Ice Crystal	2179	589
Total	4151	1128

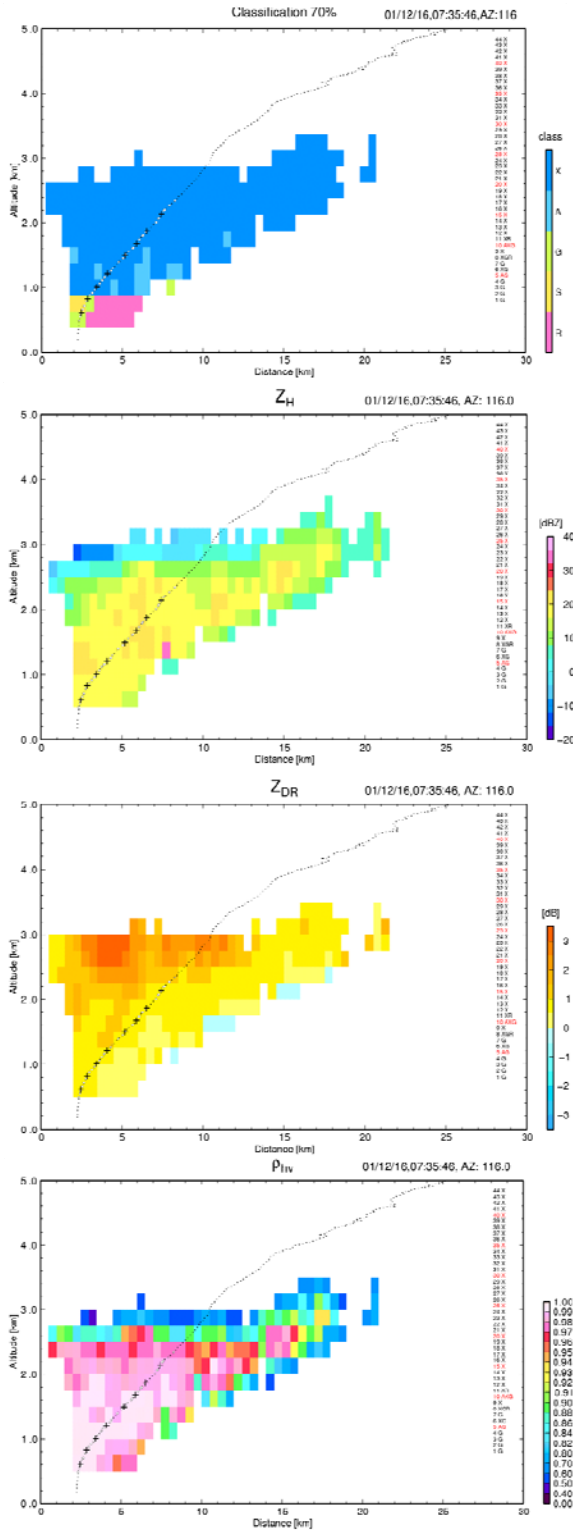
Frequency that each polarimetric parameter and air temperature has some value was derived from comparing picked-up radar and HYVIS data for each hydrometeor type.

4. Hydrometeor type classification

For hydrometeor type classification, fuzzy logic technique including a hybrid model proposed by Lim et al. (2005), which combined the additive method and the product method in the interference stage, was used. The beta membership functions, that are important for classification performance, were specified based on the derived characteristics of polarimetric measurements for each hydrometeor type described in section 3.

Figure 1 shows an example of the results of the hydrometeor type classification with the RHI images of polarimetric measurements of Z_H , Z_{DR} , and ρ_{HV} at 07:35:46 LST December 16, 2001. Each width of the beta membership function was set to the range of 70 % of accumulated frequency of polarimetric measurements and temperature from the maximum(s) to both sides.

The hydrometeor types detected by HYVIS and classified by the method were compared for validation. The rates of ‘hits’ to ‘false alarm’ for type R, S, G, A, and X were 70, 39, 58, 0, and 69 %, respectively. The reasons why it was more difficult to identify correctly aggregate (A) were considered that aggregate (A) was detected



together with the other types of hydrometeor in

Fig. 1. Hydrometeor classification result and RHI images of Z_H , Z_{DR} , and ρ_{HV} at 07:35:46 JST on Dec. 16, 2001. Dotted line, marks of open circle and cross show the HYVIS track and the positions of HYVIS image data, respectively.

almost all HYVIS images, and ice crystal (X) include originally four kinds of hydrometeors with different characteristics of particles then

with wide range of polarimetric measurements in snow clouds. The aggregate (A) and ice crystal (X) should be included in one category of dry snow at present.

5. Summary and issues

X-band polarimetric radar data were collected simultaneously as *in-situ* measurements with hydrometeor videosonde (HYVIS) in winter clouds. Both data were compared and frequency polygons of polarimetric measurements and temperature for hydrometeor types were derived. Results of hydrometeor classification using fuzzy logic technique including a hybrid rule strength (Lim et al. 2005) and its verification were also reported. The beta membership functions were specified based on the derived characteristics of polarimetric measurements and temperature for each hydrometeor type.

In-situ observation data by the Instrumented aircraft can be utilized for validation of the classification method.

Acknowledgements. The authors would like to acknowledge Dr. S.-G. Park for supporting radar observation.

References

- Iwanami, K., R. Misumi, M. Maki, T. Wakayama, K. Hata, and S. Watanabe, 2001: Development of a multiparameter radar system on mobile platform. *Proc. 30th Intern'l Conf. Radar Meteor.*, 104-106.
- Lim, S., V. Chandrasekar, and V. N. Bringi, 2005: Hydrometeor classification system using dual-polarization radar measurements: Model improvements and in situ verification. *IEEE Trans. Geosci. Remote Sensing*, **43**, 792-801.
- Liu, H., and V. Chandrasekar, 2000: Classification of hydrometeors based on polarimetric radar measurements: Development of fuzzy logic and neuron-fuzzy systems, and in situ verification. *J. Atmos. Oceanic Technol.*, **17**, 140-164.
- Murakami, M., and T. Matsuo, 1990: Development of hydrometeor videosonde. *J. Atmos. Oceanic Technol.*, **7**, 613-620.
- Zrnić, D. S., A. Ryzhkov, J. Straka, Y. Liu, and J. Vivekanandan, 2001: Testing a procedure for automatic classification of hydrometeor types. *J. Atmos. Oceanic Technol.*, **18**, 892-913.